Chapter 15

Economy of organ form and function

Christophe Goupil, Éric Herbert, Cyril Karamaoun, Benjamin Mauroy, Frédérique Noël, and Paul Ross

Chapter overview

- This chapter extends the concept of economy that previous chapters have elaborated by considering its application to the organ and the living organisms.
- The development of organs in pluricellular living organisms is conditioned by a number of factors such as nutrients, energy, and form that are here considered in the context of the economy of the organ function
- The mammalian respiratory system is subject to a high degree of constraint, primarily energetic and morphometric in nature, that played a decisive role in shaping the lung through evolutionary processes.
- The lung is the organ that is most directly responsible for respiration, a process that involves connecting the external environment to the cellular compartment through the ventilation.
- We show that the constraints on this major organ imply a high level of complexity of the organ's shape and a precise control of the ventilation.
- The scaling laws that govern the development and function of lung and are common to the entire mammalian class condition the lung's growth and determine its shape have been treated in previous works
- Through several examples, we demonstrate how these scaling i.e., *allometric* laws control the ventilation, and the respiratory processes in general.

15.1 Optimization of organs and systems

In the previous chapters, the central model of the cell has been deeply explored. On another scale, the integration of cells into larger structures such as tissues, organs, and entire systems in multicellular organisms requires an extension of the main concepts presented in this book. Nevertheless, the completion of the multiple functions of an organ follows the same general principles as for individual cells, including the economic aspects.

15.1.1 Organs and constraints

The way that a cell population aggregates itself into a high-level structure, as part of a pluricellular organism, has been determined through evolutionary processes, following a more general path of specialization of structures and functions. Each organ evolved to fulfill its functions in the most optimized manner. This observation leads us to interrogate the concept of optimization for such a large structure – from a cellular point of view. In the context of organ function, optimization can be defined through the processes by which the functions are fulfilled as best as possible while minimizing the associated cost variables. Among those variables, energy plays a central role. Thus, one possibility for constraining the organ would be to maintain its function at an optimal level while minimizing its cost in energy. This effect can be expressed mathematically. Let us define the cost in energy $\mathcal{E}$ which depends on one or

more variables $x \in \mathbb{R}^n$ ($n \geqslant 1$). Furthermore, let us define one or more equality constraints to our problem, $c(x) = 0$, where $c : \mathbb{R}^n \to \mathbb{R}^m$. The optimization problem under constraints comes down to finding an optimal value for x that minimizes the function $\mathcal{E}(x)$ while x satisfies $c(x) = 0$. This results in

$$\min_{x \in \mathbb{R}^n} \mathcal{E}(x), \text{ such that } c(x) = 0. \tag{15.1}$$

The optimization under constraint problem can be solved using the Lagrangian function,

$$\mathcal{L}(x, \lambda) = \mathcal{E}(x) - \sum_{k=1}^{m} \lambda_k c_k(x),$$

where the λ_k are Lagrange multipliers. Indeed, if we assume that x_* is the optimal solution to the problem (15.1), then thanks to the Lagrange multiplier theorem, there exists a unique Lagrange multiplier λ_* such that,

$$\nabla \mathcal{E}(x_*) = \lambda_*^T J_c(x_*),$$

where J_c is the Jacobian of the function c. It implies that the optimal solution x_* is a stationary point of $\mathcal{L}$, satisfying the condition of minimal energy expenditure.

A study of the constraints on the cardiac system offers an excellent example of energy optimization, due to high consumption of the heart. The cardiac pump delivers deoxygenated blood to the lung through pulmonary circulation and brings oxygenated blood to the whole body through systemic circulation [1]. Interestingly, blood pressure developed in both ventricles are not of the same order of magnitude, with a left ventricular pressure approximately ten times larger than the right ventricular one [1]. This makes sense from an energetic point of view; the heart requires a non-negligible amount of energy to fulfill its role of blood pumping. Furthermore, as with any mechanical system, only a fraction of the energy consumed (mainly in the form of ATP) is converted in mechanical work – around 25% [2], the rest being dissipated as heat. Thus, the pumping work tends to be optimized from an energy consumption point of view. On one hand, the pressure needed to irrigate the pulmonary circulation is low; the lung presents a small value of resistance to perfusion, and its apex is located only centimeters above the heart position. And on the other hand, the pressure developed in the systemic circulation must allow the oxygenated blood to irrigate all the organs, including high-energy consumers – muscles, brain – that located further above heart position, developing a hydrostatic pressure that the blood flow has to overcome [1]. It is to be noted that this energetic optimization is also connected to the metabolism requirements, with a pumping work closely related to the body's O_2 consumption, which ensures an optimized adaptation of the cardiac output to the body energy requirements.

Although often considered as a major aspect, this energetic constraint is far from being the only condition for a proper functioning of the organ. Other variables such as nutrient consumption, metabolic integration or physical constraints participate in shaping the organ function. Brain development in primates, and humans especially, is a prime example of effect that combination of several constraints has on energetic and nutrients availability. The underlying mechanisms that determine the evolution towards a large and complex brain structure in humans are still debated [3]. However, it is evident that the development and normal function of this organ is dependent on adequate and specific energetic and nutrients inputs. From the energetic point of view, brain metabolism largely depends on glucose consumption. However, in case of high consumption and/or deprivation, ketones metabolism takes place in order to furnish a fast and rich source of energy for the organ. Ketones are catabolized mainly in the liver [4], and have the important property of being able to cross the blood-brain barrier, to the contrary of long chains of saturated fatty acids [5]. In parallel, proper brain development and function require a large input of specific nutrients that are not common in every food source [6]. Among those, iodineand ironappear to be essential for the brain, and exert a strong constraint on its adequate growth and functioning. The notable presence of iodine-enriched food sources close to the sea shores, compared to traditional terrestrial food sources, is thought to have favored the recent development of the so-called *shore-based paradigm* of human brain evolution i.e., that the access to seafood produce supported and enhanced brain development in early hominid populations, leading to increased brain mass and cognitive functions in those populations [6]. Among these considerations, let us remind that any organ has to develop and function in specific localization and body environment. Thus, the constraints applied to an organ and its development and function can also be of morphometric nature.

15.1.2 Energy conversion in living systems

When energy is transferred to a system, its response manifests itself at the microscopic level by the excitation of its individual degrees of freedom, and at the global level when collective excitations are possible. In generic terms, a thermodynamic machine is defined as a system where an incident energy flow *dispersed* is converted into an energy flow *aggregated* and a loss flow. This conversion is performed by a thermodynamic *working fluid* which, carrying entropy, leads to a coupling between the respective potentials through the equations of state.

In the case of thermal machines, the dispersed form of energy is called heat and its associated potential is temperature, while the aggregated form is called work and its associated potential is, for example, pressure. Temperature and pressure are linked by one or more equations of state. The system response results from the collective response of the microscopic degrees of freedom of the working fluid. Thus, part of the energy received by the working fluid can be made available to a load on a global, and possibly macroscopic, scale for a given purpose as useful work, the remainder being redistributed (dispersed) at the microscopic level and dissipated due to internal friction and any other dispersion processes imposed by the boundary conditions [7]. Conversion efficiency is therefore closely related to the proportion of energy allocated to the system's collective modes.

Living organisms are open, out-of-equilibrium and dissipative systems, as they continuously exchange energy and matter with their environment [8]. Unlike classical thermodynamic engines, for which equilibrium models can be constructed using extremal principles, such a possibility does not exist in the case of living organisms due to the absence of truly identifiable equilibrium states and the absence of principle for non-equilibrium systems. Nevertheless, assuming a global system close to equilibrium, the development of a tractable thermodynamic model of metabolism can be based on notions from classical equilibrium thermodynamics. In this approach, the working fluid acts as a conversion medium, characterized by its thermoelastic properties, or chemicoelastic coefficient for chemical systems.

15.1.3 The example of the lung

As an example of an organ submitted to geometric limitations, the lung has to face, from its early development to its mature state, multiple constraints on its morphometry and proper functioning. The principal role of this organ is, as well known, to establish the connection between the respiratory gases in the atmosphere and these in circulation in the body i.e., O_2 as a reactive agent, and CO_2 as a by-product that has to be eliminated from the organism. To fulfill its role, the lung has evolved in a manner that maximizes the gas exchange surface – as diffusion is a surface phenomenon – in a reduced thoracic volume. This surface-to-volume requirement has forged the lung structure has it is known; an intricate dichotomic bronchial tree that conducts the air inwards and outwards, to and from the alveolar sacs, respectively. This semi-fractal, space-filling structure, presents the advantages of an extremely wide exchange surface enclosed in a relatively small volume [1].

The mechanisms of development of the lung branching structure in a closed environment is still a debated question [9]. Indeed, the tree structure presents a series of specific characteristics necessary for a proper functioning of the organ. Among these, the space-filling aspect of the bronchial tree is remarkable, as it solves the problem of the surface-to-volume constraint of the organ. In addition, the whole bronchial tree is a self-avoiding structure, as no bronchus enters in contact with other ones in its local environment, which ensures a proper circulation of the air in the structure. It is striking that these properties, which can be found in fractal geometries, are observed in any well-functioning lung structure, leading to important developmental questionings. For example, the pattern of branching of the bronchi, although strongly stereotyped in the first generations starting from the trachea, appears to follow a space-filling procedural development rather than a deterministic branching pattern [9]. Accordingly, some authors have developed a set of hypotheses that tend to explain these mechanisms. A group of restricted genes would encode the steps of branching and growth of the bronchi during the organ development, ensuring a proper structure of the adult lung,following procedural steps somehow encoded in genes or groups of genes coding for periodicity, bifurcating and rotating routines. However, to the best of our knowledge, these genes have not been determined nor a proper molecular mechanism of stereotypical branching.

Among the questions raised by the *programmed morphogenesis* approach, the link between the molecular dimensions and the organ world are still elusive. Another path for branching procedure, which could reconcile the deterministic

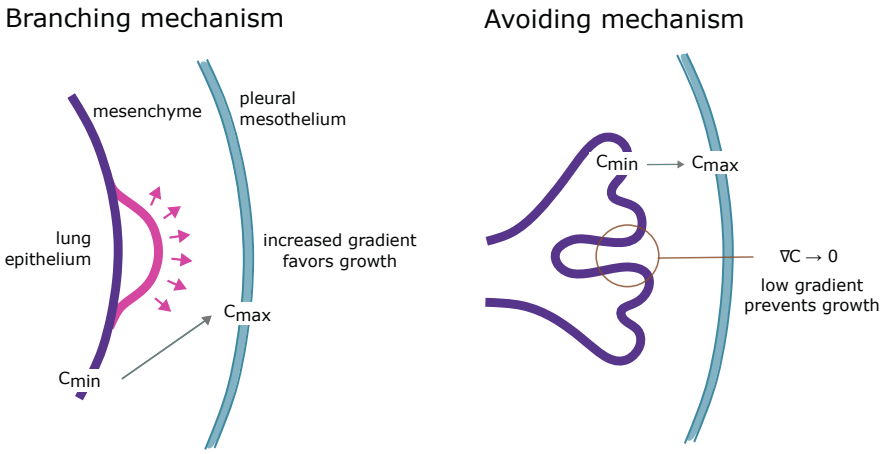

Figure 15.1: Proposed mechanism for the morphogenesis of biological branched structures – In this approach, the gradient of concentration of a key molecular activator guides the growth of specific tissue layer through the activation of the associated receptor. In this example, the local gradient of concentration of FGF10 (black arrows) activates the budding of the epithelium layer (*branching mechanism* – left). As the tissue curvature flattens, the local concentration vanishes and the growth stops, preventing the tissue overlap (*avoiding mechanism* – right) [9].

point of view with the problem of the transfer of information along different orders of magnitude is the *self-organized morphogenesis* approach. Several authors [9, 10] suggested that the branching routine of the bronchial tree is less stereotyped than thought, especially in the central and distal generations. This hypothesis is supported by the observation that modeling approaches using stochastic space-filling routines, constructed based on a stereotyped proximal tree, are capable of generating tri-dimensional branched structures that satisfy the constraints of a morphometric adult lung. On another side, the core concept of the *self-organized morphogenesis* approach relies on the observation that key molecular components are necessary and sufficient for proper growth and branching of the bronchial epithelium. Among these, the fibroblast growth factor 10 encoded by the *fgf10* gene has been demonstrated to play a central role in epithelial proliferation, whose activity is highly regulated [9].

In 2012, Clément et al. [9] proposed a scenario for the spontaneous emergence of a tree structure. This scenario is based on the sole diffusion of a protein promoting cell proliferation, such as FGF10, in an environment with two layers that mimic the bronchial epithelium and the lung mesothelium.In addition, the layers present a resistance to folding and are growing as a function of the received flow of proteins.This scenario forms a model for the lung development and has been studied using mathematical and numerical tools. To mimic the diffusion process from the outer layer of the organ (mesothelium) to the inner layer (bronchial epithelium), Clément et al. solved the Laplace equation applied on the protein concentration c:

$$\triangle c = 0$$

Then, they considered that each layer was growing according to a function of the local protein gradient:

$$\begin{aligned} \frac{d\mathbf{x}}{dt} &= f_m\left(||\nabla c(\mathbf{x})||\right) && \text{for } \mathbf{x} \text{ in the mesothelium} \\ \frac{d\mathbf{x}}{dt} &= f_e\left(||\nabla c(\mathbf{x})||\right) && \text{for } \mathbf{x} \text{ in the bronchial epithelium} \end{aligned}$$

The functions f_m and f_e are increasing functions, typically with a sigmoid shape. To avoid the epithelium to catch up with the mesothelium, f_e is kept smaller than f_m. A smoothing of the layers based on a fixed characteristic size is then performed in order to mimic the layers resistance to folding. With this model, Clément et al. observed the spontaneous formation of branching patterns similar to those observed during bronchial development, as depicted in Figure 15.1 and, based on an extended model, in Figure 15.2. Hence, this compact modeling approach is sufficient for observing *de novo* branching and growth patterns in a simulated tissular environment. Since then, this *self-organized morphogenesis* approach has been used as a framework for other organs [11] and other branched systems [12]. To date, the question of the mechanisms of development of branching organs is not clearly elucidated. However, the link between the molecular and cellular components requires further investigation, in order to unveil the determinants at

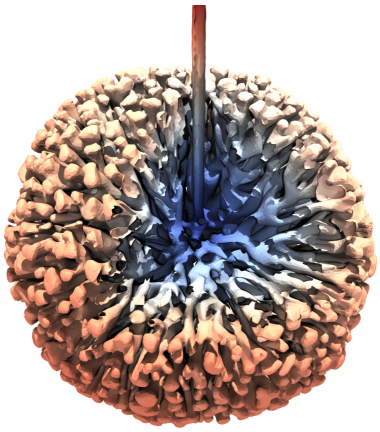

Figure 15.2: Tridimensional spontaneous emergence of a tree (*budding*) based on the model of Clément et al. (2014) [13] – An eighth of the budded sphere has been sliced out to show the branching core (blue). Notice the self-avoiding and space-filling branching, which are commonly found in biological tree structures.

the scale of the tissues and organs.

Philosophical remark 15.A The origin of shape?

How growth and organ specialization define the shape and structure of a mature organ is a long-debated scientific question that has not yet unveiled all its secrets and mysteries. Organs are rarely functional during development, at least not in the early stages. Thus, the function of an organ cannot directly drive its growth and ultimately its mature shape. So how can development build an organ that, when mature, has the correct shape and function? Evolution is the answer: if development fails to achieve a functional, efficient organ, the associated organism has little chance of being selected by evolution. But this answer raises many other questions. What is the evolutionary cost of organogenesis? What about the biological path selected by evolution for growing an organ? Is it so robust that once such a path has been selected, it renders all other paths inaccessible? Do these paths and costs form bottlenecks for the organs in terms of possible shapes, functions, and functional efficiencies? Insights into these questions will be given in Section 15.3.

However, these examples of constrained organ development raises several issues that need to be discussed in details. Among these, one can notice that the shape of the system appears as central in the developmental considerations, especially under constraints.

In the next section, the respiratory system, and the lung as its central organ, will be studied in details in light of the concepts of organ optimization. Indeed, the lung, its structure, its functioning, its efficiency, are all the result of a series of optimization under constraints that shaped the organ through evolution.

15.2 The lung as a model organ for optimization under constraints

At the core of the respiration process, the lung is the organ that connects the ambient air to the blood, allowing to transport oxygen from the ambient air to blood and carbon dioxide from blood to the ambient air. The needs of the body in oxygen and carbon dioxide, the respiratory gases, determines the lung function, which is based on a complex geometrical structure and on several physical and chemical processes.

15.2.1 Lung morphology, a complex structure

A basic description of the lung structure would consist in dividing it in two parts: the bronchial tree and the exchange surface with blood. The function of the bronchial tree is limited to the transport of the respiratory gases and no exchange occurs in this part of the lung. It forms a cascade of bifurcating airways with cylindrical shapes. There is

Physics box 15.B Energy conversion in muscles

Despite the complexity of biological systems, it is possible to apply the Onsager's phenomenological approach of locally linearized non-equilibrium thermodynamics Onsager [14]. Through this approach, it is possible to identify the non-equilibrium processes that link the degradation of the chemical potential of food by its digestion into a macroscopic form of energy made available for muscular work. By applying Onsager's approach and integrating it with macroscopic systems, we can describe the behavior of certain thermodynamic conversion machines under mixed boundary conditions [7, 15, 16]. In the case of Dirichlet boundary conditions the system is driven by the potential differences, meanwhile in Neumann boundary conditions the system is driven by the fluxes. Mixed conditions are located between these two extreme configurations. These lead to feedback effects and the emergence of complex dynamic behaviors [17].

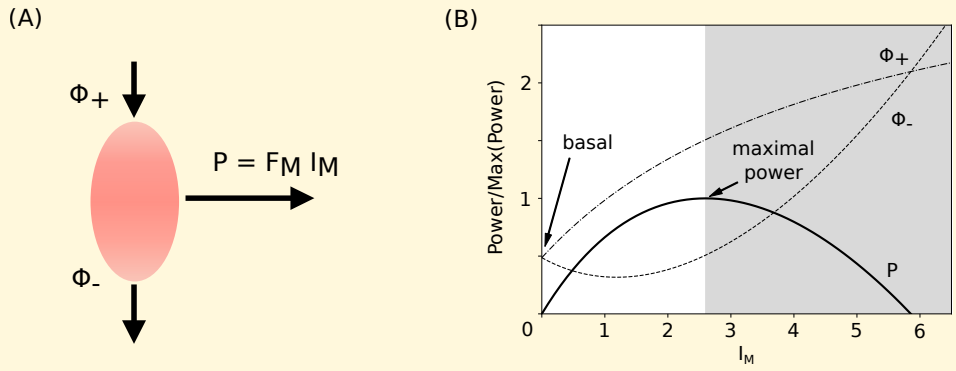

(A) Illustration of muscle as an energy converter. The incoming energy flow Φ_+ is converted into mechanical power $P = F_M I_M$ and a waste fraction Φ_-. I_M is the so-called *metabolic intensity*. (B) Plot of the system's response under varying metabolic intensities I_M. The response extends from the basal resting point to the point of exhaustion, via the point of maximum work production.

If we apply this description to the case of living organisms that have been reduced to chemical conversion machines, we obtain a thermodynamic formalism (see Figure above) that regains the phenomenological description of the muscular response proposed by Hill [18, 19]. In Hill's phenomenology, the metabolic force F_M and the contracting velocity v are linked by three constants represented by the equation $F_M = \frac{c}{v+b} - a$. The thermodynamic formulation gives $F_M = \frac{F_{iso}+R_{fb}}{I_M+I_T} I_T - (R_{fb} I_T + R_M I_M)$ where $I_M \propto v$. The thermodynamic approach gives us access to the physical meaning of the parameters i.e., F_{iso} is the isometric force of the muscle, I_T defines the threshold of acceptable metabolic intensity, R_M is the viscous resistance to displacement and R_{fb} the feedback resistance induced by the mixed conditions previously mentioned .
A proxy for the flow released by the muscle is the quantity of oxygen breathed in during ventilation [20]. To achieve an effort of a given intensity, the level of O_2 adjusts accordingly. Naturally, this quantity cannot grow indefinitely, and is limited by the absolute size of the organ that enables this exchange and by the relative size of this organ compared to the size of the individual.
For an individual, this is an intrinsic limitation on the ability to produce effort. So, depending on the size of the individual, which constrains its volume, the respiratory system must be optimized to maximize the flow of O_2. By comparing inter-species data and using a generic description, it is then possible to find an allometric law, as we shall see in this chapter.

an average of seventeen successive bifurcations in the human lung. The trunk of the tree is called the trachea; it is connected to the ambient air through the tracheo-pharyngeal pathway. The leaves of the tree are called the terminal bronchioles; they are connected to the exchange surface with blood. At each bifurcation the size of the airways is decreasing, with a tracheal diameter of about 2 cm and a diameter of the terminal bronchioles of about 0.3 to 0.5 mm. The exchange surface with blood consists in a foam-like structure that is an assembly of exchange units called the acini. Each acinus is also shaped as a bifurcating airway tree, but the size of the airways is conserved at the bifurcations. There is an average of six successive bifurcations in a typical acinus. The acinar airways are called the alveolar ducts and their walls are garnished with bubble-like structures, the alveoli. The alveoli walls are mainly blood capillaries, called pulmonary capillaries, and they are the location of the respiratory gas exchanges. Each terminal airway of the bronchial tree feeds an average of two acini. The auto-similar, multi-scaled structure of the bronchial

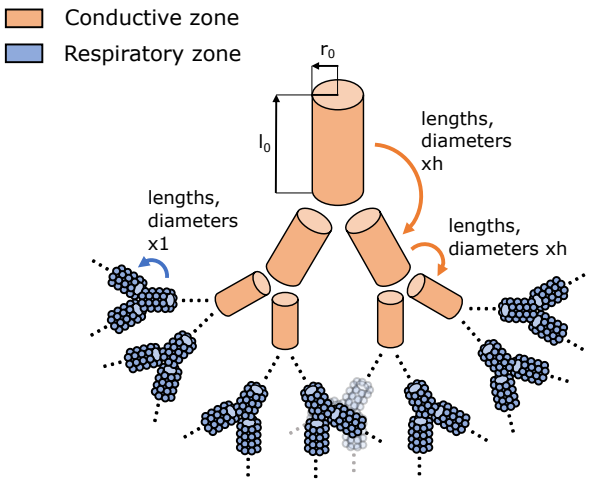

Figure 15.3: Illustration of the lung model used in this chapter – The tree in beige mimics the bronchial tree, where oxygen and carbon dioxide are only transported along the branches. The tree in blue mimics the acini, where the respiratory gases are transported along the branches. They are also captured by the alveoli that cover the walls of the branches.

tree and of the acini allows the lung to contain a very large exchange surface that is folded in the thorax. In a typical human, the exchange surface is about 70-100 m^2 [1].

Since the morphology of the lung is complex, it becomes necessary to make assumptions in order to have a simple model while conserving the principal geometrical properties. Our model is then based on the assembly of self-similar trees with cylindrical branches and symmetric bifurcations that mimic the two functional zones (see Figure 15.3). To account for the core geometrical properties of the lung, we assume that the dimensions of the branches in the conductive tree decreases from one generation to the next with a ratio $h = \left(\frac{1}{2}\right)^{\frac{1}{3}}$ [21], while in the acinus we assume that the size of the bronchi remains constant [21]. Note that the airways spatial distribution such as the branching angles or the orientations of the branching planes is not taken into account in our model since it is not really relevant for the computation of oxygen transport in the lung.

15.2.2 Lung dynamics: where physics enters the play

The transport of the respiratory gases to and from blood involves a combination of physical processes which ensure that the needs of the body in respiratory gases are fulfilled.

Diffusion : no energy costs, but too weak. As blood entering the pulmonary capillaries has an oxygen partial pressure lower than the oxygen partial pressure in the alveolar air, oxygen flows to the blood by the process of diffusion that tends to balance the partial pressures between blood and the alveolar air. For the lung's point of view, the blood acts as an oxygen sink. The transport of carbon dioxide in the lung relies on the same processes than that for oxygen, except that blood flowing in the alveoli membranes acts as a source of carbon dioxide. The diffusion process is passive in the lung i.e., no energy is spent by the organ to perform the transport. Notice that this is not true from the pulmonary blood circulation point of view, as blood has to be incessantly renewed to maintain the respiratory gas partial pressure difference between the alveolar air and the blood. However, at the metabolic time scale, the diffusion process has a limited range in the airway tree. Were the transport of the respiratory gas only based on diffusion, the lung could not maintain the respiratory gas flow at a level compatible with the mammals metabolisms. The reason behind this limitation stands in the size of the airway tree. The pathways from the ambient air to the respiratory zone are too long and narrow for the diffusion to provide gas flows compatible with the metabolism of mammals. In the case of the human lung, the typical length of these pathway is of about $L_p = 30$ cm [22]. The characteristic time t_p for an oxygen molecule to travel by diffusion through all such a pathway can be estimated using a dimensional analysis. Using L_p and the diffusion coefficient of oxygen in air $D = 0.2\ \text{cm}^2 \cdot \text{s}^{-1}$ [23], the order of magnitude of t_p can be estimated with:

$$t_p = \frac{L_p^2}{D} \simeq 4500\,\text{s} = 1 \text{ hour and } 15 \text{ minutes!}$$

Hence, a pure diffusive transport of the respiratory gas cannot fit the mammals needs. Actually, in human, the order of magnitude of the length L_D traveled by diffusion during the typical time of inspiration i.e., $t_i = 2$ seconds, is $L_D = \sqrt{D \times t_i} \simeq 6.3$ mm. Thus, in the resting human, diffusion can transport oxygen from the terminal bronchioles to the nearby exchange surface. However, at a time scale compatible with the metabolism, diffusion cannot reach the upper part of the bronchial tree. It cannot either reach the deeper parts of the respiratory zone, which is non active at rest. Actually, this last phenomenon, called the *screening effect* [23], plays a crucial role in the lung. It is described in details later in this chapter. More generally, the limited spatial range of diffusion has many consequences on the living systems. An emblematic example is its role on the size limitation of insects [24], where diffusion in the tracheal tubes is the only mean of respiratory gas transport. It participates to the explanation of why the increased atmospheric oxygen concentration during the Palaeozoic era allowed insects to be larger than today as, following Fick's law, the diffusive flow is proportional to the gradient of partial pressure between the ambient air and the inner body.

Convection : the rescuer. We have seen that the diffusion process is too weak to transport the respiratory gas through the whole airway tree. In the absence of other transport mean, the oxygen partial pressure in the lung would decrease and the flow of oxygen to blood would drop. Similarly, the carbon dioxide partial pressure would increase and prevent the exchanges with blood to occur. Consequently, the air in the lung has to be renewed in order to expel the excess of carbon dioxide and to refresh the inhaled air volume with oxygen. This phenomenon is called the ventilation. The ventilation is a dynamic i.e., time-dependent, process based on the succession of inhalation and exhalation of a volume of air, the tidal volume, at a given rate, the breathing frequency. Ventilation is performed thanks to a set of muscles that surround the lung and modify its volume. At rest regime, the main acting muscle is the diaphragm, located at the base of the lung. By first pulling onto the lung, this muscle deforms the lung tissues, creating a negative pressure drop and the transport a volume of ambient air inside the lung; this is the inspiration phase. At rest, the elastic energy stored in the tissues during the inspiration phase allows for a passive recoil of the lung and a volume of air equal to the volume inhaled is expelled; this is the expiration. Then the cycle repeats following the same procedure, at least at rest. Since the duration of a breath cycle for a resting human is about four to five seconds, a human performs, on average, about six to seven hundred millions breaths during her/his lifetime.

Modeling the oxygen transport. The transport of oxygen in the lung is then driven by three phenomena: diffusion, convection by the airflow and exchange with blood through the alveoli walls in the alveolar ducts. The partial pressure of oxygen averaged over the lumen area is transported along the longitudinal axis x of the airway. Hence, in each airway of our idealized lung, the mean partial pressure of oxygen P over the airway section follows,

$$\frac{\partial P}{\partial t} - D\frac{\partial^2 P}{\partial x^2} + u\frac{\partial P}{\partial x} = \beta\left(P_{\text{blood}} - P\right), \tag{15.2}$$

where D is the oxygen diffusion coefficient, u is the velocity of the airflow, β is a reactive term and P_{blood} is the partial pressure of oxygen in the capillary blood. The reactive term β mimics the exchanges with blood through the alveolar membrane. This coefficient depends on the diffusion coefficient of oxygen in water, on the solubility coefficient of oxygen in water, on the thickness of the alveolar-capillary membrane, and on the radius of the alveolar duct. It is equal to zero in the bronchial tree since no exchange with the blood happens in this part of the lung and is positive in the acini. The oxygen partial pressure in blood is determined by assuming that the flow of oxygen leaving an alveolar duct through the alveolar-capillary membrane is equal to the flow of oxygen captured by blood, accounting for the oxygen captured by hemoglobin and for the oxygen dissolved in plasma [1]. Finally, all generations are linked through bifurcations by assuming continuity between generations and conservation of the quantity of oxygen at each bifurcations.

15.2.3 The energy expenditure or the cost of breathing

Breathing is part of the basal metabolism, meaning that it is a regular and mandatory energy cost for the maintenance of the body. Yet, natural selection, one of the main processes driving evolution, tends to select for minimal energetic cost so that the organisms can allocate most of their resources to their reproduction. Hence, in order to understand breathing, it is important to determine the origin of the energetic costs and how they are affected by the breathing process. We already pointed out that diffusion, considered from the lung point of view, is a passive process. So, most of the energetic costs involved in the lung function arise from the process of ventilation. Energy is spent through the

Math box 15.C Conditions for the numerical simulations

Our model takes as input the ventilation parameters: the tidal volume V_T (in mL) and the breathing frequency f_b (in min^{-1}) and outputs the mean amount of oxygen exchanged with blood over a respiratory cycle. To validate our model, we performed computations at rest by assuming that a human breathes around 12 times per minute and inhales around 500 mL of air for each breathing cycle. With these parameters, our transport model gives an oxygen flow exchanged with blood of 230 mL $\cdot$ min^{-1}, which is close to the average physiological value of 250 mL $\cdot$ min^{-1} [1].

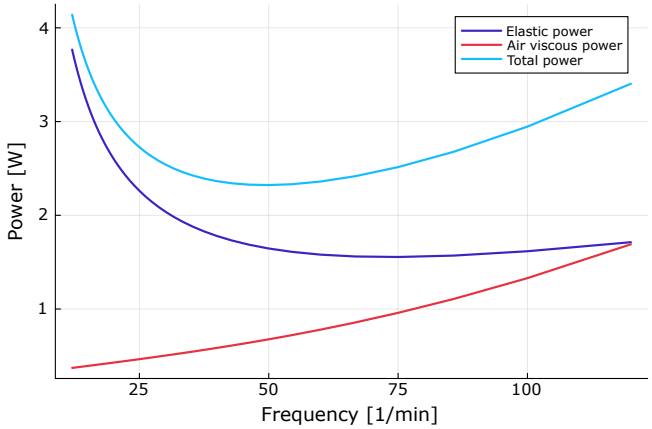

Figure 15.4: Trade-off between elastic energy stored in the tissue and viscous energy dissipated in the air circulation (exercise regime, computed from our model).

action of the muscles on the lung. This action has two main effects: it deforms the tissues and it displaces the air along the bronchial tree. On the one hand, the tissues are deformed due to the action of the thoracic muscles, especially the diaphragm. This deformation is considered as elastic in the normal range of ventilation [25], and energy is dissipated along the displacement of the tissues. On the other hand, as every gas, air acts as a fluid with specific viscosity. As the bronchial tree is an assembly of a high number of narrow tubes with decreasing size, the energy spent for the displacement of the air in the bronchial tree is dominated by the energy dissipated by the friction of air in the bronchi. The air kinetic energy is negligible relatively to the dissipation. This can be summarized in term of the power spent by the muscles (energy per unit of time):

$$\underbrace{\mathcal{P}_{\text{m}}}_{\text{muscle power}} \simeq \underbrace{\mathcal{P}_{\text{e}}}_{\text{elastic power}} + \underbrace{\mathcal{P}_{\text{a}}}_{\text{air viscous dissipation}} .$$

These quantities depend on several lung characteristics, on the breathing frequency f and on the amount of air inhaled during on breath cycle V_T. This raises the trade-off shown in Figure 15.4 and, using optimization theory, optimal ventilation frequencies and tidal volume can be be predicted. The viscous dissipation of air in the bronchial tree is characterized by the lung hydrodynamic resistance $\mathcal{R}$, which is directly related to the geometry, size, number and structuring of the bronchi [25]. The hydrodynamic resistance is a physical quantity that represents how the energy put in the system is divided between kinetic energy and heat energy. It connects the volume of air displaced per unit of time, also called air flow F, to the force per unit of surface applied to the air, also called air pressure p_a: $p = \mathcal{R}F$. For the same pressure applied on the lung, the higher the hydrodynamic resistance, the lower the air flow and the higher the dissipation. Then, the power dissipated by viscous friction of the air inside all the bronchi can be estimated by $\mathcal{P}_{\text{a}} = pF = \mathcal{R}F^2$. By assuming in our case that the velocity of the air follows a sinus function, we can deduce the power dissipated by viscous friction as follows:

$$\mathcal{P}_{\text{a}} = \frac{1}{4}\mathcal{R}\left(\pi f_b V_T\right)^2 ,$$

where $\mathcal{R}$ is the hydrodynamic resistance, f_b the respiratory frequency and V_T the tidal volume.

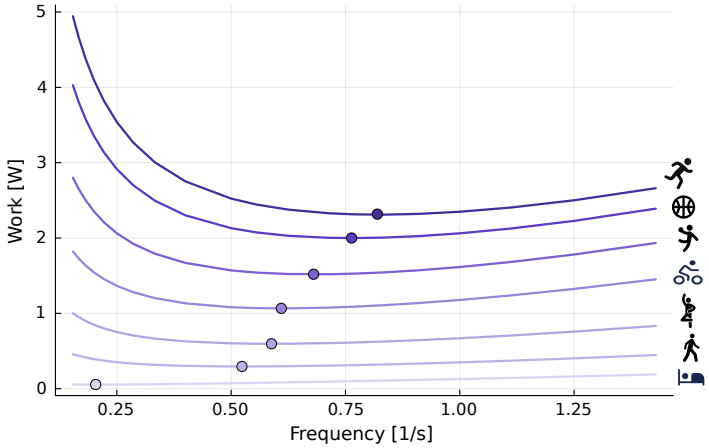

Figure 15.5: Total power expenditure during ventilation (W) as a function of the respiratory frequency (s^{-1}) for different intensities of exercise – Dots correspond to the optimal ventilation frequency i.e., that minimizes the dissipated power. Adapted from [28].

The elastic power is characterized by the compliance $\mathcal{C}$ of the lung, that relates the force per unit of surface applied by the muscles (p_m) to the volume change of the lung [26]. The compliance depends on the lung's volume, especially when the deformation of the lung is high although the compliance can be considered constant while healthy. That is why, in our case, we assume that the compliance is a constant and we neglect the non-linearities arising at large lung's deformations [27]. The elastic power can be estimated by integration of the volume along the inspiration phase and it gives us,

$$\mathcal{P}_{\mathrm{e}} = \frac{V_T^2 f_b}{2\mathcal{C}},$$

where $\mathcal{C}$ is the compliance of the lung previously defined. Finally, the total energetic cost of breathing $\mathcal{P}$ can be written as the sum of the power dissipated by viscous friction $\mathcal{P}_{\mathrm{a}}$ and the elastic power $\mathcal{P}_{\mathrm{e}}$. The total power has to be minimized relatively to the tidal volume V_T and the breathing frequency f_b with a constraint on the oxygen flow to blood that has to match the oxygen flow demand (see Equation 15.1). Thanks to our model previously defined, we can compute the oxygen flow to blood as a function of tidal volume and breathing frequency and compare it to the oxygen flow $\dot{V}_{\mathrm{O}_2}$ requested by the body at the regime considered.

Our model predicts (see Figure 15.5), for a human at rest, an optimal breathing frequency of 12.2 breaths per minute and an optimal tidal volume of 497 mL, which are very close to the average physiological values [29]. The model exhibits a robustness in term of frequency perturbation around the optimal. A 5% shift in the energy brings the frequency into a range between 8 breaths per minute up to 18.5 breaths per minute. This effect is due to the fact that, at low regimes, a low tidal volume V_T is sufficient to perform an optimal ventilation. When the exercise intensity increases, the power profiles as a function of the frequency become steeper and steeper and focus the optimal value within a tighter region. It implies that a shift from the optimal configuration at high intensities is predicted to be costly in term of energy spent. This behavior is fully compatible with the fact that the control of ventilation is stronger at exercise, preventing even talking. The question of the optimal conditions of ventilation in human leads naturally to a series of extensions that need to be considered. We have seen previously that the optimization under constraints occurs in almost every organ in all the living beings. Thus, could we expect the present model to be extended to all mammals, as the control of ventilation is, more than probably, present in the whole mammalian class?

15.3 Allometric scaling laws for respiration and ventilation

The answer to this question of generalization leads us to a vast scientific question that will bring us back to the late 19$^{\text{th}}$ century and which is still open on many aspects.

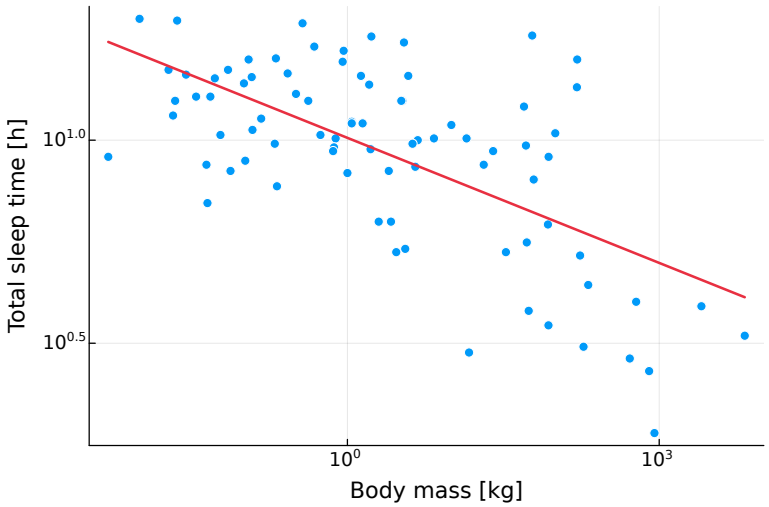

Figure 15.6: Distribution of total sleep duration (S) in mammals – The plot is based on data from Savage & West [30]. The data is best fitted by the red curve which represents the corresponding allometric relation $S = 10.1 \times M^{-0.103}$.

15.3.1 The emergence of scaling relations in nature

In 2007, Savage and West published a seminal work in which they present a collection of data of sleep duration in a set of mammalian species. Among other major results, their analysis confirmed the previous observation that the larger the animal, the shorter the duration of its sleep cycle [30]. More precisely, the sleep duration correlates negatively with the body mass of the mammal and follows, based on the data from Savage & West, an interesting exponential law of the form $t_s = 10.1\, M^{-0.103}$, with t_s the sleep duration in hours during a 24 hours period and M the body mass of the mammal in kilograms, as seen in Figure 15.6 [30]. Thus, by taking the logarithm of both sides of the equation, one can write this sleep-to-mass relation as log t_s = log 10.1 - 0.103 log M i.e., a linear relation between the logarithm of the sleep duration and the logarithm of the mass of the animal, see Figure 15.6. As we will see later, this type of exponential relation is now referred, in ecological sciences, as an *allometric* scaling. In general, an allometric law will write $Y = Y_0 M^b$, where Y is the studied – physiological, morphometric – property, M the mass of the living organism, Y_0 and b the allometric prefactor and exponent, respectively [31]. Actually, the concept presented by Savage & West is far from being recent. The history of the study of allometric relations dates back to the 19$^{\text{th}}$ century. Scientists from various disciplines started to analyze the changes in shape and form of living beings in relation with their overall size.

15.3.2 A brief history of allometry

In a pioneer work from 1897, Eugène Dubois described the relation that guides the evolution of brain's mass and that of the individual in a variety of mammal species [32]. He observed that brain is smaller, relatively to the their mass, in bigger animals. He then derived an adequate expression for this relation, such as $e = c\, s^r$, where e is the brain's mass, s the body mass and c and r two coefficient that define the relation, with r close to 1/2, justifying the relative decrease in brain's mass that he observed. As far as we know, this represents the first mathematical expression of an allometric law, years before this term was even coined as it. It is in 1907 that Lapicque [33] had the idea to transform Dubois' relation in a log-log dependency, giving a straight line representation in logarithmic coordinates that is now familiar to us, cf. Figure 15.6. At that time, this work was purely descriptive and empirical. However, biological and ecological data started to accumulate in the following years that led, mainly in animal species, to a variety of scaling laws. Thus, the ubiquity of allometric relations in every ecological discipline raised the question of the nature of the biological mechanisms underlying their observation.

In parallel, the question of the emergence of forms in living organisms arose in the literature. One of the major works at that time came from the Scottish naturalist D'Arcy Wentworth Thompson, whose main contribution came from his book *On Growth and Form*, first published in 1917 [34]. In this publication, he adopted the – still debated – thesis that the living systems as we know are submitted, in addition to the process of natural selection, to the physical laws of

nature that can modify, transform and adapt their form and their path of development i.e., their growth. This reference publication paved the way to the new disciplinary research field of biomathematics and, even in present times, is still considered as a major contribution to this field. However, the D'Arcy Thompson's approach has not been accepted by the whole community, and the debate is still vivid more than a century after the publication of the first edition of his work [35]. Indeed, D'Arcy Thompson was not entirely convinced by the pure Darwinian approach that dominated the field of developmental biology in his time. Although a strong Darwin's admirer, he rather considered that the paths of development of the organisms were not dictated purely by acquired mutations and hard-encoded routines. At the contrary, he was convinced that these paths could only follow a number of sequences, a series of schemes that, following the laws of physics and chemistry, would allow for the formation of the variety of shapes and developments observed in nature [36]. Critics emerged about his teleological – in some ways – conception of evolution, or at least of emergence of form. In essence, his work was one of his time, and his theories of forces of development were not supported by the genetic and molecular knowledge that has since been accumulated [35]. D'Arcy Thompson was an author of his time. He paved the way, with others developmental naturalists, to numerous concepts in biomathematics that influenced a number of past and present works, as discussed in Section 15.1. But D'Arcy Thompson was also an author among his peers. Motivated by his conception of developmental shaping forces, he started to correspond with a younger British naturalist named Julian Huxley, who will later forge a prolific international career as a biologist and science advocate, although carrying with him some controversies that are beyond the scope of this chapter.

The scientific correspondence started slightly after one of Huxley's major publication, dated from 1924. In this article, Huxley studied the dynamics of growth of chelae in a crab species whose individuals possess one small and one large chela [37]. What seems at first a highly specific topic is enlarged by the idea to measure the mass of the chelae *relatively* to the mass of the individual. Following the steps of Dubois and Lapicque, Huxley weighted around 400 specimens of crab and plotted in a logarithmic scale the mass of the large chela against the total weight of the animal minus the weight of the large chela. He then observed that the experimental data could be joined by a straight line in this logarithmic plot. The originality of Huxley's work resides in his interpretation of the results that he obtained. He noticed that the slope k of the regression line remained larger than one, in accordance with the observation of the relative larger i.e., heterogonic growth of the chela compared to the growth of each individual. He then provided a proposed mechanism for this relative growth: the rate of cellular division in the chela is larger than the one in the rest of the body, more precisely in a $k : 1$ ratio [37]. With this – still emergent – mechanistic approach, Huxley provided for the first time a simple method for deciphering heterogonic growth of a characteristic, that will be observed as a straight line of slope $k > 1$ when plotted against the normalized mass of the individual in logarithmic coordinates.

Finally, the works of Lapicque, Dubois, D'Arcy Thompson and all their contemporaries emerged in 1936 in a joint paper between Huxley and a younger scientist, Georges Teissier, in which they agreed for the terminology of *allometry* and the associated law that is now famous $y = bx^{\alpha}$ [38]. Altogether, this brief section on the historical emergence of the allometric concept in ecological sciences depicts a vibrant and active research theme, developed in the late 19^{th} century, which extends the Darwinian concept of natural selection towards the emergence of growth, form and function. However, the reader will notice that the allometric approach of these times is still largely descriptive, with limited causal explanations of the nature of the scaling coefficients and the putative mechanisms that drive their behavior.

15.3.3 Allometry: a mechanistic approach

Many years later, a possible approach that compensates for this lack of mechanistic causality would be found in the work of West, Brown and Enquist (*WBE*), published in 1997 [31]. In this major article, the authors focused on the allometries in metabolic properties that have been described in the past decades, with the aim of developing a new mechanistic framework that would explain these allometries i.e., be able to derive the allometric exponents for the numerous physiological properties at stake here. The question of the existence of a general allometry for the metabolic rate of the living beings is a thrilling question. This would imply that all the organisms, from the tiny bacteria to the massive trees or mammals, do possess shared mechanisms of energy expenditure that would reflect on the presence of a common exponent all over the different orders of magnitudes among the species. Furthermore, the exponent should reflect somehow, by its value, the nature of the energetic mechanisms, and thus could be derived by a comprehensive modeling approach. WBE answer positively to these strong hypotheses, and developed a structured approach

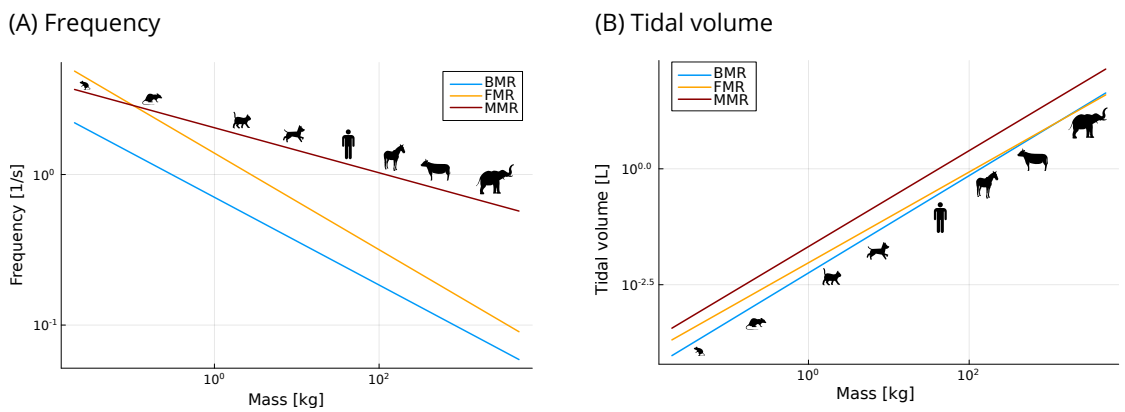

Figure 15.7: Scaling laws for lung usage – Predicted ventilation frequency (s^{-1} – *left*) and tidal volume (L – *right*) as a function of the mammal mass (kg – log-log scale) at different metabolic regimes. BMR: Basal Metabolic Rate, FMR: Field Metabolic Rate, MMR: Maximal Metabolic Rate.

that focuses on the modeling of energy and mass fluxes in biological networks – cardiovascular and respiratory systems for example – which they consider as the common ground for all the species [31]. The hypotheses of WBE are of strong nature, and have been discussed largely in the literature (see for example [39]. Although this important – and still open – debate lies beyond the scope of this chapter, it appears important to emphasize that the WBE approach created a mechanistic, mathematical framework for the study of allometric relations that, somehow, acted as a bridge between the traditional descriptive allometry and the modern mechanistic approach.

15.3.4 Allometric relations for the respiratory system

As far as the respiratory system is concerned, the model of WBE appears to act as a promising framework for the study of the allometric relations of this system [40]. Indeed, the lungs of mammals are built as a network of mass and energy transfer, as described before, and share morphological and functional properties, raising the question on whether the previous results for human can be extended or not to all mammals. These properties are known to be dependent on the mass M of the mammal with allometric scaling laws [31, 38]. Furthermore, the physics of ventilation, and hence its control, is linked to the geometry of the lung. Consequently, the morphological differences among mammals also affect the control of ventilation.

First, our gas transport model for the human lung presented in the previous section can be slightly modified to be valid for all mammals. Indeed, we know that the lungs of mammals share invariant characteristics [29] such as the tree-like structure with bifurcating branches and the decomposition into two parts: the bronchial tree and the acini. The derivation of a lung model that depends only on mammal mass requires to relate explicitly the morphological parameters involved in our model such as the tracheal radius and length, with the animal mass. We used the datasets from [31]. The oxygen transport and exchange now occur in the idealized lung that has been generalized to fit any mammal. The transport of oxygen in the mammals lung is still driven by the tree phenomena: convection by the airflow, diffusion and exchange with blood through the alveoli walls. Hence, in each airway, the partial pressure of oxygen follows the convection-diffusion-reaction equation (15.2) previously defined. The exchange coefficient β is dependent on the mammals mass since it depends on the radius of the alveolar duct which follows an allometric law. Finally, we search for the minimum of the total energetic cost of breathing $\mathcal{P}$ relatively to the tidal volume V_T and the breathing frequency f_b with a constraint on the oxygen flow to blood that has to match the oxygen flow demand $\dot{V}_{O_2}$. Since allometric scaling laws for oxygen flow demands for mammals at basal, field and maximal metabolic rates are available in the literature [41, 42, 43, 44], we can compute the desired oxygen flow $\dot{V}_{O_2}$ depending on the mammal mass and on the metabolic regime.

Our model predicts that breathing frequencies and tidal volumes follow indeed allometric scaling laws. Furthermore, these laws can be derived in three different metabolic regimes: basal metabolic rate (BMR), field metabolic rate (FMR)

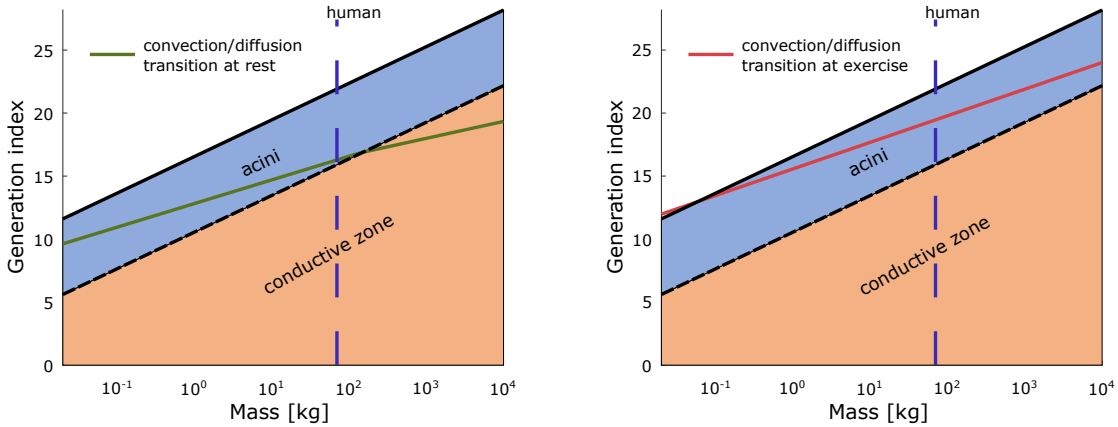

Figure 15.8: Localization in terms of lung generation index of the conductive zone and of the exchange surface (acini) as a function of the mammal species mass (kg) – Both the green line (rest regime – *left*) and the red line (maximal exercise regime – *right*) represent the transition from a transport of the respiratory gas by convection to a transport by diffusion. Adapted from [40].

and maximal metabolic rate (MMR), as seen in Figure 15.7,

$$f_b^{\text{BMR}} \approx 0.61\, M^{-0.27}\ \text{Hz},\ V_T^{\text{BMR}} \approx 6.1\, M^{1.04}\text{mL},$$
$$f_b^{\text{FMR}} \approx 1.17\, M^{-0.31}\ \text{Hz},\ V_T^{\text{FMR}} \approx 11.8\, M^{0.97}\text{mL},$$
$$f_b^{\text{MMR}} \approx 1.37\, M^{-0.17}\ \text{Hz},\ V_T^{\text{MMR}} \approx 29.7\, M^{1.01}\text{mL}.$$

It predicts exponents that are in accordance with the values observed in the literature. Indeed, breathing rate at BMR has been estimated to follow the law $f_b^{\text{BMR}} \simeq 0.58\ M^{-\frac{1}{4}}$ Hz [45] and tidal volume to follow the law $V_T^{\text{BMR}} \simeq 7.14\ M^1$ mL [31]. At other metabolic rates, less data is available in the literature except for the breathing rate of mammals at MMR, estimated to follow the law $f_b^{\text{MMR}} \simeq 5.08\ M^{-0.14}$ Hz [46]. The validation of our model at both minimal and maximal metabolic regimes suggests that its predictions should be coherent whatever the regime, in the limit of the availability of its input parameters. This indicates that the mechanical power spent for ventilation might have driven the selection by evolution of the ventilation patterns.

The idealized representation of the bronchial tree and of the exchange surface used in this study accounts for five core characteristics common to all the mammals lungs, as identified in the literature [29, 22, 28, 31]: a bifurcating tree structure; an homogeneous decrease of the size of the bronchi at the bifurcations; the size of the trachea; the size of the alveoli; and the surface area of the exchange surface. These characteristics are the main determinants for the tuning of the ventilation in order to minimize its energetic cost. This indicates that once the metabolic regime is fixed, the morphology of the lung is probably the primary driver of the physiological control of ventilation. We tested this hypothesis by altering, in our analysis, the allometric scaling laws related to the geometry of the lung. We observed corresponding alteration of the laws predicted for tidal volumes and breathing frequencies. Since morphology itself has probably been selected by evolution in order to minimize the hydrodynamic resistance in a constrained volume [22], morphology and ventilation patterns are intertwined together in order for the lung to function with a low global energetic cost i.e., a low hydrodynamic resistance R and a low ventilation cost $\mathcal{P}(V_T, f_b)$ that also depends on R. Interestingly, our representation of the lung does not account for interspecific differences known to exist between the lungs of mammals, such as different degrees of branching asymmetry, monopodial or bipodial lungs, etc. [47].

As in the human lung, the transport of gases in the mammalian lung relies on the two major processes of diffusion and convection. We know that, in humans, the diffusive transport in the alveolar ducts is submitted to a physical phenomenon called the *screening effect* [23]. Indeed, as gas exchanges occur through the alveoli walls lining the alveolar ducts, the diffusion can transport the respiratory gases only on a limited range of generations. This range depends on the physico-chemical properties affecting the diffusion of the gas in the alveolar air and through the alveolo-capillary membrane. This range has been estimated to be of about four generations for oxygen and one for carbon dioxide [23] in humans. The description of the screening effect in mammals requires several additional hypotheses. Because of

Physics box 15.D The cost of oxygen transport

The allometric relationship found applies to the pulmonary organ. This is a crucial link in muscular activity, and therefore in locomotion or any activity requiring an effort, even moderate. As such, its properties must also be present during physical exercise. A useful quantity, based on oxygen consumption $\dot{V}_{O_2}$ and frequently used in the literature, is the Cost of Oxygen Transport (COT). This corresponds to the ratio $\dot{V}_{O_2}/v$ with v the locomotion velocity. Using the correct metabolic conversion factor COT is the energy dissipated per unit length. It is known empirically that COT shows a local minimum corresponding to an optimal situation in which the minimum energy is dissipated per unit length. Building on this property, Tucker in 1975 [48] noted that this minimum follows distinct allometric laws according to the major locomotion families, runners, swimmers and fliers, see the Figure below.

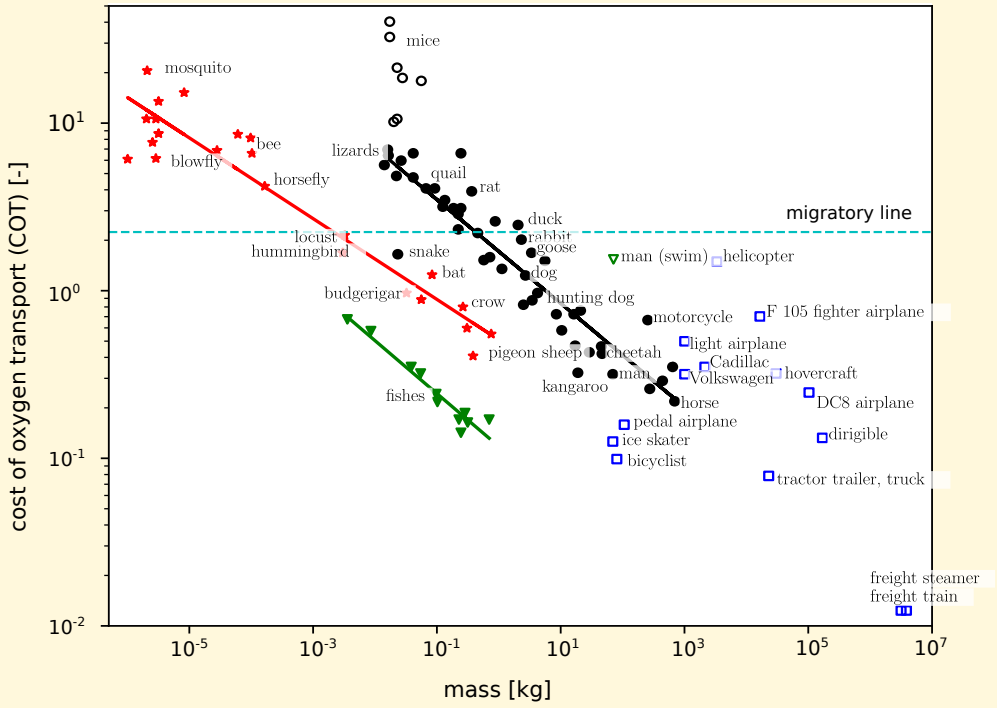

The COT is defined here as the ratio $P/(M\,v)$, with P the power production and v the velocity as a function of the body mass M for several species (adapted from [48]). Green are swimmers, red are fliers, black are runners, blue are engines designed by engineers. Continuous lines correspond to linear fits on data shown with filled markers.

the screening effect, the alveolar ducts far from the convection–diffusion transition get only a small diffusive oxygen flow, as most of the available oxygen has been captured by the alveolar ducts closer to the transition. In these deep parts of the acini, the oxygen partial pressure gradient between the deoxygenated blood and the alveolar ducts, which drives the oxygen capture by blood, is low. Carbon dioxide is mostly evacuated from the alveolar ducts very close to the transition: they are refilled by carbon dioxide too quickly for the deeper ducts to be drained of gas by diffusion. Hence, the ducts far from the transition cannot be relieved of the carbon dioxide and the exchange with blood in these ducts is low. As a consequence, the deeper part of the exchange surface is not available for the exchanges. The location of the transition between convective and diffusive transport of the respiratory gas drives the magnitude of the screening, and this transition depends on the geometry of the airway tree and of the ventilation regime. The screening phenomenon in mammals has been studied mathematically in [40]. Within the framework of the models hypotheses, the authors show that the number of conductive airways N_{conD} and the number of alveolar ducts N_{ad} follow allometric scaling laws:

$$N_{\mathrm{conD}} \propto N_{\mathrm{ad}} \propto M^{\frac{7}{8}}.$$

Additionally, they show that the number of airways N_{conV} in which the gases are transported by convection also

Physics box 15.E The cost of oxygen transport as a function of speed

In walking or running animals, the cost of oxygen transport (see Box 15.D) depends on an animal's speed, as shown in the figure on the right. On top is oxygen consumption $\dot{V}_{O_2}$ of a horse plotted against the speed $v/v^\star$ for walk (red stars), trot (blue dots), and gallop (green squares), and their fits with our modeling. Bottom is COT for the same set of data. The three gaits data are normalized by the muscle fiber ratio leading to a unique master curve.

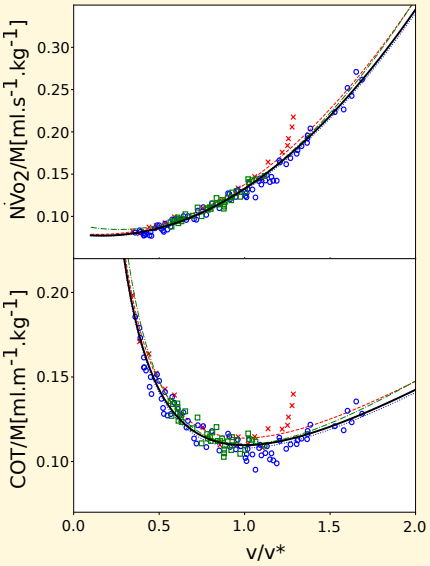

Based on the model proposed in Box "Energy conversion", it has been demonstrated that a living system can be described as a collection of N identical, *standard*, muscle units operating in parallel [49]. Then the COT expression becomes:

$$\text{COT} \quad = \quad \frac{N}{N_H}\left(a_0\, k + r_M\, k^2\, v + \frac{b}{v}\right) \qquad (15.3)$$

with $a_0\, k$ a constant, r_M a dissipative term and b the basal consumption i.e., out of effort. This last three parameters describing the standard muscle unit.

We are then allowed to derive the minimum of the COT as an intrinsic property of energy conversion machines, $\text{COT}_{\min} \propto \sqrt{r_M\, b}$. It is found independent of the number of standard muscle fibers involved in the effort. Thus, effort is a combination of the number N of standard muscle fibers used and their characteristics b and r_M. The parameterization of the standard muscle fiber depends on the specific implementations for an organism. It can be expected to be identical for a single animal. We have carried out this work in the case of the horse, which exhibits three well-differentiated gaits: walk, trot and gallop (see the Figure above. We show that the COT curves, or equivalently $\dot{V}_{O_2}$, of the different gaits can be found using N as the only adjustable parameter, leaving the muscle fiber parameters unchanged.

As muscle is the most common means of producing power in animals, the typical behavior described here should be found in the most general way, without barriers between species, genera or classes. Of course, muscular implementation is specific to each animal, constrained by its own characteristics (intensity of effort, size, etc.), which suggests the origin of the observed scaling laws.

follows an allometric scaling law. This law depends on the ventilation regime:

$$N_{\text{conV}} \propto \begin{cases} \begin{cases} M^{0.56} & \text{if } M < 150 \text{ kg} \\ M^{0.405} & \text{if } M \geq 150 \text{ kg} \end{cases} & \text{at rest} \\ M^{0.63} & \text{at maximal exercise} \end{cases}$$

These equations translate into linear relationships in terms of $\log(M)$, as shown in Figure 15.8. Rest regime is represented on the left plot and maximal exercise regime on the right plot. The figure indicates that, at rest regime, the small mammals use their lung very efficiently, as only a few of their acini generations are fed by diffusion, as indicated by the green curve in Figure 15.8. Hence, the screening effect in small mammals is weak. However, this suggests that they have few reserve for increasing their metabolism at exercise [23, 40]. As suggested by the red curve on the right plot in Figure 15.8, the shift of the transition between convection and diffusion to deeper generations does not increase significantly the available exchange surface. To the contrary, large mammals are submitted to large screening effects at rest regime, and a large part of their exchange surface is not used. However, during exercise, the shift of the transition towards a deeper lung generation allows to recruit a significantly larger exchange surface.

It is to be noted that the predictions of our model for the localization of the convection–diffusion transition in idealized lungs lead to good estimations of the allometric scaling laws for tidal volumes and breathing frequencies, indicating that the morphological parameters included in our model might drive primarily the control of ventilation.

Through this short introduction to allometry of constrained organs, we started to decipher the latent mechanisms

of development of a constrained organ inside a class of organisms. The example of the lung is emblematic: how a complex and central organ can develop, specialize and evolve to fulfill the needs of organisms, while sharing among species its particularities, and efficiency.

15.4 Concluding remarks

Biological optimization, making the most effective use of limited resources within a set of given constraints, is a multifaceted subject that has been a source of content for countless articles and a stimulus for related discussion. To make the optimization of biological systems more readily comprehensible, this chapter has focused attention on a single organ, the human lung, and used it as a stage on which to introduce basic principles and a canvas on which to illustrate their application. The range of constraints, for the most part energetic or morphometric in nature, that have conditioned the development of the lung over the long course of its evolutionary history and given the mammalian respiratory system its particular shape is expansive. The characteristics of these constraints and the conditions that govern their interplay can be represented as mathematical equations that form the basis for models that describe the scale of the effect constraints have on biological systems and illuminate the magnitude of their impact. The insights into the lung's form that these models yield also provide a more thorough understanding of its function, characterizing, for example, modulations in the regulation of respiratory ventilation that occur in response to changes in the body's state – e.g., when the body is at rest or in motion; when it is healthy or when its health is compromised. The models are also a source of results that can be abstracted and subsequently applied to both human organs and those of other species that are larger and more complex. Considered within this broader context, they can also be seen as integral elements of much larger systems and as instances of the general allometric laws to which those systems adhere. The significance of the larger orthogenetic and phylogenetic implications that this abstraction of specific models into generalized laws carries cannot be overstated and discussion of those implications is vigorous and far-reaching. Through these discussions, many aspects of allometry have been illuminated and a deeper understanding of the complex systems that determine the ways individuals, species and systems function and interact has been achieved. Yet many of the field's underlying mechanisms and governing principles remain to be discovered. This chapter is the prelude to a journey into a space at the intersection of biology, ecology, and mathematics that the allometric universe occupies and the fuel for the exploration of the mysteries those hidden mechanisms are waiting to reveal.

Recommended readings

- For a proper introduction to respiratory physiology, in healthy and pathological conditions: John B. West, *Respiratory Physiology: The Essentials* [1].
- A reading for a deeper understanding of the lung morphometry: Ewald R. Weibel, *Morphometry of the human lung* [21] and one for the respiratory gases exchange: Ewald R. Weibel, *The Pathway for Oxygen: Structure and Function in the Mammalian Respiratory System* [29].
- A nice thesis about (in)organic mechanisms of morphogenesis: Raphaël Clément, *Morphogénèse et développement pulmonaire* [50].
- The old but gold textbook in morphogenesis of living beings: D'Arcy Wentworth Thompson, *On Growth and Form* [34].
- On allometric relations, in general: Robert H. Peters, *The Ecological Implications of Body Size* [41] and from a modeling approach: G. B. West et al., *A general model for the origin of allometric scaling laws in biology* [31].

Problems

Problem 15.1

Recover the expression of the power dissipated by viscous friction $\mathcal{P}_a$ and the elastic power $\mathcal{P}_e$ while assuming that:

- the air velocity is a sine function,
- the power obtained is a mean value over inspiration.

Hint: The instantaneous elastic power is written as follow,

$$\mathcal{P}_e = \frac{1}{\mathcal{C}} V(t) F(t),$$

where $\mathcal{C}$ is the compliance of the lung, $V(t)$ is the volume of the lung and $F(t)$ is the air flow.

Problem 15.2

The localization of the transition between convective and diffusive transport can be estimated with the Péclet number. This number measures the relative influence of the transport of oxygen by convection on the transport by diffusion. It depends on the generation and can be written as follow,

$$Pe_i(t) = \frac{l_i u_i(t)}{D},$$

where l_i is the length of the bronchi of generation i, $u_i(t)$ is the air velocity, and D is the diffusion coefficient.

(a) Compute the average of the time-dependent Péclet number $Pe_i(t)$ over a half breath cycle while assuming that,
- the length of the bronchi of generation i depends on the length of the trachea as follow : $l_i = l_0 h^i$,
- the air velocity in generation i depends on the air velocity in the trachea as follow, $u_i(t) = u_0(t)\left(2h^2\right)^{-i}$,
- u_0 is a sine function,
- the tidal volume is the integral over the inspiration of the product of the cross section of the trachea and the velocity of the air, $V_T = \int_0^{T/2} \pi r_0^2 u_0(t) dt$.

The expected expression is :

$$Pe_i = \frac{2V_T f_b l_0}{\pi r_0^2 D}\left(\frac{1}{2h}\right)^i.$$

(b) The generation k at which the transition between convection and diffusion occurs is computed by solving the equation Pe_k = 1. Compute the value 2^k for which Pe_k = 1.

Bibliography

[1] John B. West. *Respiratory Physiology: The Essentials*. Lippincott Williams and Wilkins, Philadelphia, 9th revised edition edition, August 2011. ISBN 978-1-60913-640-6.

[2] Paul Knaapen, Tjeerd Germans, Juhani Knuuti, Walter J. Paulus, Pieter A. Dijkmans, Cornelis P. Allaart, Adriaan A. Lammertsma, and Frans C. Visser. Myocardial energetics and efficiency: current status of the noninvasive approach. *Circulation*, 115(7):918–927, February 2007. ISSN 1524-4539. doi: 10.1161/CIRCULATIONAHA.106.660639.

[3] R. I. M. Dunbar and Susanne Shultz. Why are there so many explanations for primate brain evolution? *Philos Trans R Soc Lond B Biol Sci*, 372(1727):20160244, August 2017. ISSN 1471-2970. doi: 10.1098/rstb.2016.0244.

[4] David G. Cotter, Rebecca C. Schugar, and Peter A. Crawford. Ketone body metabolism and cardiovascular disease. *Am J Physiol Heart Circ Physiol*, 304(8):H1060–1076, April 2013. ISSN 1522-1539. doi: 10.1152/ajpheart.00646.2012.

[5] Ryan W. Mitchell and Grant M. Hatch. Fatty acid transport into the brain: of fatty acid fables and lipid tails. *Prostaglandins Leukot Essent Fatty Acids*, 85(5):293–302, November 2011. ISSN 1532-2823. doi: 10.1016/j.plefa.2011.04.007.

[6] Stephen C. Cunnane and Michael A. Crawford. Energetic and nutritional constraints on infant brain development: implications for brain expansion during human evolution. *J Hum Evol*, 77:88–98, December 2014. ISSN 1095-8606. doi: 10.1016/j.jhevol.2014.05.001.

[7] M. V. Volkenshtein. *Biophysics*. Mir Publishers, 1983. ISBN 978-0-12-723150-1.

[8] P. Glansdorff and Ilya Prigogine. *Thermodynamic Theory of Structure, Stability and Fluctuations*. Wiley-Interscience, 1971. ISBN 978-0-471-30280-3. doi: 10.1002/bbpc.19720760520.

[9] Raphaël Clément, Pierre Blanc, Benjamin Mauroy, Vincent Sapin, and Stéphane Douady. Shape self-regulation in early lung morphogenesis. *PLoS ONE*, 7(5):e36925, 2012. ISSN 1932-6203. doi: 10.1371/journal.pone.0036925.

[10] Pierre Blanc, Karen Coste, Pierre Pouchin, Jean-Marc Azaïs, Loïc Blanchon, Denis Gallot, and Vincent Sapin. A role for mesenchyme dynamics in mouse lung branching morphogenesis. *PLoS One*, 7(7):e41643, 2012. ISSN 1932-6203. doi: 10.1371/journal.pone.0041643.

[11] Denis Menshykau, Odyssé Michos, Christine Lang, Lisa Conrad, Andrew P. McMahon, and Dagmar Iber. Image-based modeling of kidney branching morphogenesis reveals GDNF-RET based Turing-type mechanism and pattern-modulating WNT11 feedback. *Nat Commun*, 10(1):239, January 2019. ISSN 2041-1723. doi: 10.1038/s41467-018-08212-8.

[12] G. Facchini, A. Lazarescu, A. Perna, and S. Douady. A growth model driven by curvature reproduces geometric features of arboreal termite nests. *J R Soc Interface*, 17(168):20200093, July 2020. ISSN 1742-5662. doi: 10.1098/rsif.2020.0093.

[13] Raphaël Clément and Benjamin Mauroy. An archetypal mechanism for branching organogenesis. *Phys Biol*, 11 (1):016003, February 2014. ISSN 1478-3975. doi: 10.1088/1478-3975/11/1/016003.

[14] H. Ouerdane, Y. Apertet, C. Goupil, and Ph. Lecoeur. Continuity and boundary conditions in thermodynamics: From Carnot's efficiency to efficiencies at maximum power. *The European Physical Journal Special Topics*, 224(5): 839–864, July 2015. ISSN 1951-6401. doi: 10.1140/epjst/e2015-02431-x.

[15] A. L. Demain and A. Fang. The natural functions of secondary metabolites. *Advances in Biochemical Engineering/Biotechnology*, 69:1–39, 2000. ISSN 0724-6145. doi: 10.1007/3-540-44964-7_1.

[16] Lev A. Blumenfeld. *Problems of Biological Physics*. Springer Berlin Heidelberg, January 1981. ISBN 978-3-540-10401-8.

[17] Marko Jusup, Tânia Sousa, Tiago Domingos, Velimir Labinac, Nina Marn, Zhen Wang, and Tin Klanjšček. Physics of metabolic organization. *Physics of Life Reviews*, 20:1–39, March 2017. ISSN 1873-1457. doi: 10.1016/j.plrev.2016.09.001.

[18] Hill Archibald Vivian. The heat of shortening and the dynamic constants of muscle. *Proc. R. Soc. Lond. B Biol. Sci.*, 126(843):136–195, October 1938. doi: 10.1098/rspb.1938.0050.

[19] Christophe Goupil, Henni Ouerdane, Eric Herbert, Clémence Goupil, and Yves D'Angelo. Thermodynamics of metabolic energy conversion under muscle load. *New Journal of Physics*, 21(2):023021, February 2019. ISSN 1367-2630. doi: 10.1088/1367-2630/ab0223.

[20] Xingbo Yang, Matthias Heinemann, Jonathon Howard, Greg Huber, Srividya Iyer-Biswas, Guillaume Le Treut, Michael Lynch, Kristi L. Montooth, Daniel J. Needleman, Simone Pigolotti, Jonathan Rodenfels, Pierre Ronceray, Sadasivan Shankar, Iman Tavassoly, Shashi Thutupalli, Denis V. Titov, Jin Wang, and Peter J. Foster. Physical bioenergetics: Energy fluxes, budgets, and constraints in cells. *Proc. Natl. Acad. Sci. U.S.A.*, 118(26):e2026786118, June 2021. doi: 10.1073/pnas.2026786118.

[21] Ewald R. Weibel. *Morphometry of the human lung*. Academic Press, 1963.

[22] B. Mauroy, M. Filoche, E. R. Weibel, and B. Sapoval. An optimal bronchial tree may be dangerous. *Nature*, 427 (6975):633–636, February 2004. ISSN 1476-4687. doi: 10.1038/nature02287.

[23] Bernard Sapoval, M. Filoche, and E. R. Weibel. Smaller is better–but not too small: a physical scale for the design of the mammalian pulmonary acinus. *Proc. Natl. Acad. Sci. U.S.A.*, 99(16):10411–10416, August 2002. ISSN 0027-8424. doi: 10.1073/pnas.122352499.

[24] Jon F. Harrison, Alexander Kaiser, and John M. VandenBrooks. Atmospheric oxygen level and the evolution of insect body size. *Proceedings of the Royal Society B: Biological Sciences*, 277(1690):1937–1946, March 2010. doi: 10.1098/rspb.2010.0001.

[25] Bertrand Maury. *The Respiratory System in Equations*. Number 7 in MS&A - Modeling, Simulations & Applications. Springer-Verlag, 2013. doi: 10.1007/978-88-470-5214-7.

[26] Jonathan Stephano. *Conséquences de l'asymétrie et de la compliance des bronches sur les propriétés hydrodynamiques du poumon, applications à la kinésithérapie respiratoire*. PhD thesis, Université Côte d'Azur, May 2021. URL https://hal.science/tel-03239006v4.

[27] Frédérique Noël. *Influence de la ventilation sur les propriétés de transport dans un poumon sain et enflammé*. PhD thesis, 2021. URL http://www.theses.fr/2021COAZ4004. Université Côte d'Azur.

[28] Frédérique Noël and Benjamin Mauroy. Interplay Between Optimal Ventilation and Gas Transport in a Model of the Human Lung. *Front Physiol*, 10:488, 2019. ISSN 1664-042X. doi: 10.3389/fphys.2019.00488.

[29] Ewald R. Weibel. *The Pathway for Oxygen: Structure and Function in the Mammalian Respiratory System*. Harvard University Press, 1984. ISBN 978-0-674-65791-5.

[30] Van M. Savage and Geoffrey B. West. A quantitative, theoretical framework for understanding mammalian sleep. *Proceedings of the National Academy of Sciences*, 104(3):1051–1056, January 2007. doi: 10.1073/pnas.0610080104. Publisher: Proceedings of the National Academy of Sciences.

[31] G. B. West, J. H. Brown, and B. J. Enquist. A general model for the origin of allometric scaling laws in biology. *Science*, 276(5309):122–126, April 1997. ISSN 0036-8075. doi: 10.1126/science.276.5309.122.

[32] Eugène Dubois. *Bulletins de la Société d'anthropologie de Paris*. 1897.

[33] Louis Lapicque. *Bulletins de la Société d'anthropologie de Paris*. 1907.

[34] D'Arcy Wentworth Thompson. *On Growth and Form*. Canto. Cambridge University Press, Cambridge, 1992. doi: 10.1017/CBO9781107325852.

[35] Maurizio Esposito. Problematic "Idiosyncrasies": Rediscovering the Historical Context of D'Arcy Wentworth Thompson's Science of Form. *Science in Context*, 27(1):79–107, March 2014. ISSN 0269-8897, 1474-0664. doi: 10.1017/S0269889713000392. Publisher: Cambridge University Press.

[36] James Briscoe and Anna Kicheva. The physics of development 100 years after D'Arcy Thompson's "On Growth and Form". *Mechanisms of Development*, 145:26–31, June 2017. ISSN 1872-6356. doi: 10.1016/j.mod.2017.03.005.

[37] Julian S. Huxley. Constant Differential Growth-Ratios and their Significance. *Nature*, 114(2877):895–896, December 1924. ISSN 1476-4687. doi: 10.1038/114895a0.

[38] J. S. Huxley and G. Teissier. Terminology of Relative Growth. *Nature*, 137(3471):780–781, May 1936. ISSN 1476-4687. doi: 10.1038/137780b0.

[39] J. Kozłowski and M. Konarzewski. Is West, Brown and Enquist's model of allometric scaling mathematically correct and biologically relevant? *Functional Ecology*, 18(2):283–289, 2004. ISSN 1365-2435. doi: 10.1111/j.0269-8463.2004.00830.x.

[40] Frédérique Noël, Cyril Karamaoun, Jerome A. Dempsey, and Benjamin Mauroy. The origin of the allometric scaling of lung ventilation in mammals. *Peer Community Journal*, 2, 2022. ISSN 2804-3871. doi: 10.24072/pcjournal.76.

[41] Robert H. Peters. *The Ecological Implications of Body Size*. Cambridge University Press, March 1986. ISBN 978-0-521-28886-6. doi: 10.1017/CBO9780511608551.

[42] M. Kleiber. Body size and metabolism. *Hilgardia*, 6(11):315–353, January 1932. ISSN 0073-2230. doi: 10.3733/hilg.v06n11p315.

[43] Lawrence N. Hudson, Nick J. B. Isaac, and Daniel C. Reuman. The relationship between body mass and field metabolic rate among individual birds and mammals. *Journal of Animal Ecology*, 82(5):1009–1020, 2013. ISSN 1365-2656. doi: 10.1111/1365-2656.12086.

[44] Ewald R. Weibel and Hans Hoppeler. Exercise-induced maximal metabolic rate scales with muscle aerobic capacity. *Journal of Experimental Biology*, 208(9):1635–1644, May 2005. ISSN 0022-0949, 1477-9145. doi: 10.1242/jeb.01548.

[45] J. Worthington, I. S. Young, and J. D. Altringham. The relationship between body mass and ventilation rate in mammals. *Journal of Experimental Biology*, 161(1):533–536, November 1991. doi: 10.1242/jeb.161.1.533.

[46] J. D. Altringham and I. S. Young. Power output and the frequency of oscillatory work in mammalian diaphragm muscle: the effects of animal size. *Journal of Experimental Biology*, 157(1):381–389, May 1991. ISSN 0022-0949, 1477-9145. doi: 0.1242/jeb.157.1.381.

[47] Benjamin Mauroy and Plamen Bokov. The influence of variability on the optimal shape of an airway tree branching asymmetrically. *Phys Biol*, 7(1):16007, 2010. ISSN 1478-3975. doi: 10.1088/1478-3975/7/1/016007.

[48] V. A. Tucker. The Energetic Cost of Moving About: Walking and running are extremely inefficient forms of locomotion. Much greater efficiency is achieved by birds, fish—and bicyclists. *American Scientist*, 63(4):413–419, 1975. ISSN 0003-0996. doi: 10.1016/0010-406X(70)91006-6.

[49] E. Herbert, H. Ouerdane, Ph. Lecoeur, V. Bels, and Ch. Goupil. Thermodynamics of Animal Locomotion. *Physical Review Letters*, 125(22):228102, November 2020. doi: 10.1103/PhysRevLett.125.228102. Publisher: American Physical Society.

[50] Raphaël Clément. *Morphogénèse et développement pulmonaire*. PhD thesis, Paris 7, January 2011. URL https://theses.hal.science/tel-00585972.